

A STATICALLY COMPATIBLE LAYERWISE STRESS APPROACH FOR MULTILAYERED MATERIALS

Rawad Baroud^{1,2}, Karam Sab¹, Jean-Francois Caron¹, Fouad Kaddah², Wassim Raphael²

¹Université Paris-Est, Laboratoire Navier (UMR 8205 CNRS, ENPC, IFSTTAR), 77455
Marne-la-Vallée, France

Emails: rawad@rawadbaroud.com & karam.sab@enpc.fr & caron@enpc.fr

²Université Saint Joseph, Ecole Supérieure d'Ingénieurs Beyrouth, Centre Libanais d'Études et de
Recherches de la Construction, Mar Roukoz - Dekwaneh, Lebanon
Emails: fouad.kaddah@usj.edu.lb & wassim.rafael@usj.edu.lb

Keywords: Multilayer, Free edge, Layerwise model, Finite element, Interlaminar stresses

Abstract

This paper presents a new layerwise model for multilayered plates, named *SCLSI*, as an abbreviation of Statically Compatible Layerwise Stresses with first-order membrane stress approximations per layer in thickness direction. The new model is derived by means of the minimum of complementary energy principle and is designed to exactly comply with free-edge boundary conditions. As in the *LSI* model proposed in [1], the laminated plate is considered as a superposition of Reissner plates coupled by interfacial stresses which are considered as generalized stresses. However, the divergences of the interlaminar transverse shears are introduced as additional generalized stresses in the *SCLSI* model. In order to get enhanced *LSI* and *SCLSI* models, a refinement strategy through the thickness is applied by considering several mathematical layers per physical layer. The refined *SCLSI* model increases the accuracy of the non refined model near singularities. A new version of an in-house finite element program called MPFEAP, based on *SCLSI* model, is developed using an 8-node with $6n-1$ d.o.f. per node (n : total number of layers). The new model shows itself very effective as shown by several comparisons between the predictions of *LSI*, *SCLSI*, their refined versions and Abaqus full 3D FE for straight free edge plate under uniaxial tension.

1. Introduction

It is well-known that multilayered materials with anisotropic layers exhibit stress concentration at the interfaces between layers, especially at the vicinity of free edges. Indeed, this is due to the large difference in anisotropy of two consecutive plies, inducing damage such as delamination in cross-ply laminates. These singularities make usual 3D Finite Element (FE) calculations very costly in calculation time, and potentially non-converging and mesh dependent. Inspired by Pagano's model [2], an alternative model to 3D FE was proposed in [1, 3–11]. In this model, the multilayered material is considered as a superposition of Reissner-Mindlin plates coupled together by interlaminar stresses which are considered as additional generalized stresses. This model has been used to study the local responses of multilayered composites, especially at the interface between layers. In order to make reference to Carrera's nomenclature proposed in [12], this model previously called *Multi-particle Model of Multilayered Materials (M4)* was renamed as *LSI* which means a Layerwise Stress approach with first-order membrane stress approximations per layer in thickness direction. The *LSI* model that shows efficiency in representing edges effects and singularities in inter- and intra-layers, calculates complex 3D multilayers using 2D

plane mesh and has been validated by 3D FE and comparisons with analytical solutions. In addition to the foregoing, a refined *LSI* model was presented in [9] by introducing several *mathematical layers* per physical layer in order to capture the stress concentrations occurring in delaminated multilayered plates under uniaxial tension. It was proved that the proposed layerwise mesh strategy improves considerably stress and energy release rate estimations given by the non refined *LSI* model [8]. Nevertheless, the non refined *LSI* model shows itself very effective in the simulation of mode I (Double Cantilever) and mode II (End Notched Flexure) delamination tests on multilayered plates [10], and in the simulation of delamination propagation in multilayered materials at $0^\circ/\theta^\circ$ interfaces [11].

Although the *LSI* model and its refined version are very powerful and effective models, several improvements can be still achieved. Without a doubt, the 3D stress free boundary conditions cannot be precisely met by these models, and besides, as these models are derived by mean of the Hellinger-Reissner mixed variational principle, there is no theoretical guarantee of the convergence of the *refined LSI* model to the 3D model, as the number of mathematical layers per physical layer increases. So as to enhance the *LSI* model, a new layerwise model called *Statically Compatible LSI (SCLSI)*, is presented where the laminated plate is still considered as a superposition of Reissner plates coupled by interlaminar stresses. However, the divergences of the interlaminar transverse shears are considered as additional generalized efforts. The new model is determined by means of the minimum of the complementary potential energy guaranteeing the convergence of its refined version to the exact 3D model, as the number of mathematical layers per physical layer increases. Besides, the new model has been implemented in a new version of the in-house FE code *MPFEAP (MultiParticle Finite Element Analysis Program)*.

The construction of the *SCLSI* model will be summarily described in the next section. In order to validate this model, a numerical example corresponding to a free edge plate under uniaxial tension will be presented and comparisons will be made between *LSI*, *SCLSI*, *refined LSI*, *refined SCLSI* and full 3D FE models.

2. Theoretical formulation of the statically compatible model *SCLSI*

In this section, a new model for multilayered plates named *SCLSI* is described. The *SCLSI* model is derived from the 3D exact model by considering Statically Compatible Layerwise Stresses with first-order membrane stress approximations per layer in the thickness direction. The generalized stresses of the proposed model are Reissner-Mindlin plate's stresses per layer in addition to interlaminar shear and normal stresses at the interfaces between layers and the divergences of the interlaminar shear stresses. The detailed description of the model can be found in [13].

2.1. Static

The basic assumption of the model is to consider in-plane stresses which are layerwise linear in the thickness direction, z . As a consequence of this assumption and 3D equilibrium equations, the out-of-plane stresses become necessarily layerwise parabolic in z for transverse shears, and layerwise cubic in z for normal stresses. Taking into account the continuity of the out-of-plane stresses at the interfaces between layers, it can be shown that the stresses fields in layer i , for $1 \leq i \leq n$, are necessarily of the form:

$$\sigma_{\alpha\beta}^{3D}(x, y, z) = N_{\alpha\beta}^i(x, y) \frac{P_0^i(z)}{e^i} + \frac{12}{e^{i^2}} M_{\alpha\beta}^i(x, y) P_1^i(z) \quad (1)$$

$$\begin{aligned} \sigma_{\alpha 3}^{3D}(x, y, z) = & Q_{\alpha}^i(x, y) \frac{P_0^i(z)}{e^i} + \left(\tau_{\alpha}^{i,i+1}(x, y) - \tau_{\alpha}^{i-1,i}(x, y) \right) P_1^i(z) + \\ & \left(Q_{\alpha}^i(x, y) - \frac{e^i}{2} \left(\tau_{\alpha}^{i,i+1}(x, y) + \tau_{\alpha}^{i-1,i}(x, y) \right) \right) \frac{P_2^i(z)}{e^i} \end{aligned} \quad (2)$$

$$\begin{aligned} \sigma_{33}^{3D}(x, y, z) = & \left(\frac{1}{2} (v^{i,i+1}(x, y) + v^{i-1,i}(x, y)) + \frac{e^i}{12} (\pi^{i,i+1}(x, y) - \pi^{i-1,i}(x, y)) \right) P_0^i(z) + \\ & \left(\frac{e^i}{10} (\pi^{i,i+1}(x, y) + \pi^{i-1,i}(x, y)) + \frac{6}{5} (v^{i,i+1}(x, y) - v^{i-1,i}(x, y)) \right) P_1^i(z) + \\ & \frac{e^i}{12} (\pi^{i,i+1}(x, y) - \pi^{i-1,i}(x, y)) P_2^i(z) + \\ & \left(\frac{e^i}{2} (\pi^{i,i+1}(x, y) + \pi^{i-1,i}(x, y)) + (v^{i,i+1}(x, y) - v^{i-1,i}(x, y)) \right) P_3^i(z) \end{aligned} \quad (3)$$

Here, the superscripts i and $j, j + 1$ indicate layer i and the interface between layer j and $j+1$ with $1 \leq i \leq n$ and $1 \leq j \leq n - 1$, respectively. By extension, the superscript 0, 1 refers to the lower face of the plate and the superscript $n, n + 1$ refers to its upper face. Greek subscripts $\alpha, \beta, \gamma, \delta, \dots$ indicate the in-plane components (x, y) and go through 1, 2. Latin subscripts k, l, m, n, \dots indicate the components (x, y, z) and go through 1, 2, 3. $N_{\alpha\beta}^i, M_{\alpha\beta}^i$ and Q_α^i are generalized stresses associated to layer i , $\tau_\alpha^{i,i+1}, v^{i,i+1}$ and $\pi^{i,i+1}$ are generalized stresses associated to the interface between layers i and $i + 1$. The polynomials $P_k^i, k = 0, 1, 2, 3$, are the orthogonal Legendre-like polynomial basis defined on layer i for $h_i^- \leq z \leq h_i^+$:

$$\begin{cases} P_0^i(z) = 1 \\ P_1^i(z) = \frac{z - \bar{h}_i}{e^i} \\ P_2^i(z) = -6 \left(\frac{z - \bar{h}_i}{e^i} \right)^2 + \frac{1}{2} \\ P_3^i(z) = -2 \left(\frac{z - \bar{h}_i}{e^i} \right)^3 + \frac{3}{10} \left(\frac{z - \bar{h}_i}{e^i} \right) \end{cases} \quad (4)$$

where in each layer i , h_i^-, h_i^+ and \bar{h}_i are, respectively, the bottom, the top and the mid-plane z coordinates of the layer, and $e_i = h_i^+ - h_i^-$ is its thickness. Hence, we have $h_{i+1}^- = h_i^+$ for all $1 \leq i \leq n - 1$. By convention, we set $h_0^+ = h_1^-$ and $h_{n+1}^- = h_n^+$.

Reciprocally, the generalized stresses can be obtained from the 3D stresses by the following formulas:

$$\begin{aligned} N_{\alpha\beta}^i(x, y) &= \int_{h_i^-}^{h_i^+} \sigma_{\alpha\beta}^{3D}(x, y, z) dz \\ M_{\alpha\beta}^i(x, y) &= \int_{h_i^-}^{h_i^+} (z - \bar{h}_i) \sigma_{\alpha\beta}^{3D}(x, y, z) dz \\ Q_\alpha^i(x, y) &= \int_{h_i^-}^{h_i^+} \sigma_{\alpha 3}^{3D}(x, y, z) dz \\ \tau_\alpha^{j,j+1}(x, y) &= \sigma_{\alpha 3}^{3D}(x, y, h_j^+) = \sigma_{\alpha 3}^{3D}(x, y, h_{j+1}^-) \\ v^{j,j+1}(x, y) &= \sigma_{33}^{3D}(x, y, h_j^+) = \sigma_{33}^{3D}(x, y, h_{j+1}^-) \end{aligned} \quad (5)$$

Note that, unlike all the other introduced generalized stresses, $\pi^{j,j+1}$ defined on the interface between layer j and layer $j + 1$ is a new generalized stress which was not considered in the *LSI* model.

2.2. Kinematics

It is obtained by writing the weak form of the statical compatibility conditions on σ^{3D} :

$$\int_{\Omega} \sigma_{kl,l}^{3D} u_k dx dy dz = 0 \quad (6)$$

The generalized displacements are defined as follows, where $i = 1, \dots, n$ and $j = 1, \dots, n - 1$:

$$U_\alpha^i(x, y) = \int_{h_i^-}^{h_i^+} \frac{P_0^i(z)}{e^i} u_\alpha(x, y, z) dz, \quad (7)$$

$$\Phi_{\alpha}^i(x, y) = \int_{h_i^-}^{h_i^+} \frac{12}{e^{i2}} P_1^i(z) u_{\alpha}(x, y, z) dz, \quad (8)$$

$$U_3^i(x, y) = \int_{h_i^-}^{h_i^+} \left(\frac{P_0^i(z)}{e^i} + \frac{P_2^i(z)}{e^i} \right) u_3(x, y, z) dz, \quad (9)$$

$$W_{\pm}^i(x, y) = \int_{h_i^-}^{h_i^+} \left(P_1^i(z) \pm \frac{P_2^i(z)}{2} \right) u_3(x, y, z) dz \quad (10)$$

$$V^{j,j+1}(x, y) = W_{-}^j(x, y) - W_{+}^{j+1}(x, y) \quad (11)$$

$U_{\alpha}^i(x, y)$, $U_3^i(x, y)$, $\Phi_{\alpha}^i(x, y)$ are the five Reissner-Mindlin generalized displacements of layer i already introduced in the *LSI* model: respectively, the two in-plane displacements, the vertical displacement and the two bending rotations. In contrast, $V^{j,j+1}(x, y)$ is a new kinematical variable, having the dimension of an area, which is dual of the static variable $\pi^{j,j+1}(x, y)$ defined on interface $j, j + 1$. The generalized strains dual of the generalized stresses $N_{\alpha\beta}^i, M_{\alpha\beta}^i, Q_{\alpha}^i, \tau_{\alpha}^{j,j+1}, \nu^{j,j+1}, \pi^{j,j+1}$ for $i = 1, \dots, n$ and $j = 1, \dots, n - 1$ are respectively calculated in terms of the generalized displacements as:

$$\begin{aligned} \varepsilon_{\alpha\beta}^i &= \frac{1}{2} (U_{\alpha,\beta}^i + U_{\beta,\alpha}^i), \\ \chi_{\alpha\beta}^i &= \frac{1}{2} (\Phi_{\alpha,\beta}^i + \Phi_{\beta,\alpha}^i), \\ \gamma_{\alpha}^i &= \Phi_{\alpha}^i + U_{3,\alpha}^i, \\ D_{\alpha}^{j,j+1} &= U_{\alpha}^{j+1} - U_{\alpha}^j - \frac{e^j}{2} \Phi_{\alpha}^j - \frac{e^{j+1}}{2} \Phi_{\alpha}^{j+1} + V_{,\alpha}^{j,j+1}, \\ D_{\nu}^{j,j+1} &= U_3^{j+1} - U_3^j, \\ \lambda^{j,j+1} &= V^{j,j+1}. \end{aligned} \quad (12)$$

2.3. Constitutive equations

The generalized constitutive equations of the *SCLSI* model that link the generalized stresses to the generalized strains are derived by using the stress energy formulation. Assuming that the fourth-order compliance tensor of layer i , $\mathbf{S}^i = (S_{klmn}^i)$, is monoclinic in direction z : $S_{\alpha\beta\gamma 3}^i = S_{\alpha 3\beta 3}^i = 0$, we obtain the following membranar, bending and transverse shear constitutive equations of layer i , respectively,

$$\varepsilon_{\alpha\beta}^i = \frac{1}{e^i} S_{\alpha\beta\gamma\delta}^i N_{\gamma\delta}^i + S_{\alpha\beta 33}^i \left(\frac{1}{4} (\nu^{i,i+1} + \nu^{i-1,i}) + \frac{e^i}{24} (\pi^{i,i+1} - \pi^{i-1,i}) \right) \quad (13)$$

$$\chi_{\alpha\beta}^i = \frac{12}{e^{i3}} S_{\alpha\beta\gamma\delta}^i M_{\gamma\delta}^i + \frac{1}{e^i} S_{\alpha\beta 33}^i \left(\frac{3}{5} (\nu^{i,i+1} - \nu^{i-1,i}) + \frac{e^i}{20} (\pi^{i,i+1} + \pi^{i-1,i}) \right) \quad (14)$$

$$\gamma_{\alpha}^i = \frac{6}{5e^i} S_{\alpha\beta 33}^i Q_{\beta}^i - \frac{1}{10} S_{\alpha\beta 33}^i (\tau_{\beta}^{i,i+1} + \tau_{\beta}^{i-1,i}) \quad (15)$$

and the following shear, normal and for the π generalized stress constitutive equations of interface $j, j + 1$, respectively,

$$\begin{aligned} D_{\alpha}^{j,j+1} &= -\frac{1}{10} S_{\alpha\beta 33}^j Q_{\beta}^j - \frac{1}{10} S_{\alpha\beta 33}^{j+1} Q_{\beta}^{j+1} - \frac{e^j}{30} S_{\alpha\beta 33}^j \tau_{\beta}^{j-1,j} \\ &+ \frac{2}{15} (e^j S_{\alpha\beta 33}^j + e^{j+1} S_{\alpha\beta 33}^{j+1}) \tau_{\beta}^{j,j+1} - \frac{e^{j+1}}{30} S_{\alpha\beta 33}^{j+1} \tau_{\beta}^{j+1,j+2} \end{aligned} \quad (16)$$

$$D_v^{j,j+1} = \frac{9}{70} e^j S_{3333}^j v^{j-1,j} + \frac{13}{35} (e^j S_{3333}^j + e^{j+1} S_{3333}^{j+1}) v^{j,j+1} + \frac{9}{70} e^{j+1} S_{3333}^{j+1} v^{j+1,j+2} - \frac{13}{420} (e^j)^2 S_{3333}^j \pi^{j-1,j} + \frac{11}{210} ((e^j)^2 S_{3333}^j - (e^{j+1})^2 S_{3333}^{j+1}) \pi^{j,j+1} + \frac{13}{420} (e^{j+1})^2 S_{3333}^{j+1} \pi^{j+1,j+2} \quad (17)$$

$$+ \frac{1}{4} S_{\alpha\beta 33}^j N_{\alpha\beta}^j + \frac{1}{4} S_{\alpha\beta 33}^{j+1} N_{\alpha\beta}^{j+1} + \frac{3}{5e^j} S_{\alpha\beta 33}^j M_{\alpha\beta}^j - \frac{3}{5e^{j+1}} S_{\alpha\beta 33}^{j+1} M_{\alpha\beta}^{j+1}$$

$$\lambda^{j,j+1} = -\frac{1}{140} (e^j)^3 S_{3333}^j \pi^{j-1,j} + \frac{1}{105} ((e^j)^3 S_{3333}^j + (e^{j+1})^3 S_{3333}^{j+1}) \pi^{j,j+1} - \frac{1}{140} (e^{j+1})^3 S_{3333}^{j+1} \pi^{j+1,j+2} + \frac{13}{420} (e^j)^2 S_{3333}^j v^{j-1,j} + \frac{11}{210} ((e^j)^2 S_{3333}^j - (e^{j+1})^2 S_{3333}^{j+1}) v^{j,j+1} - \frac{13}{420} (e^{j+1})^2 S_{3333}^{j+1} v^{j+1,j+2} \quad (18)$$

$$+ \frac{1}{24} e^j S_{\alpha\beta 33}^j N_{\alpha\beta}^j - \frac{1}{24} e^{j+1} S_{\alpha\beta 33}^{j+1} N_{\alpha\beta}^{j+1} + \frac{1}{20} S_{\alpha\beta 33}^j M_{\alpha\beta}^j + \frac{1}{20} S_{\alpha\beta 33}^{j+1} M_{\alpha\beta}^{j+1}$$

2.4. The refined SCLSI model as a static discretization of the 3D model

The *refined SCLSI* is obtained by discretizing each physical layer in p mathematical layers as shown in Fig. 1, for a total of np mathematical layers, then the new *refined SCLSI model* will be a better approximation of the real 3D stress field than the non refined *SCLSI*. As the number p of mathematical layers per physical layer increases, the results will asymptotically coincide with the exact 3D stress field. An irregular discretization of the physical layers is adopted in order to better describe the stress concentration at the interfaces between the physical layers as proposed in [9]. As shown in Fig.1, the layerwise mesh strategy in the thickness direction is in the form of a geometric progression, where h_{min} is the thickness of the mathematical layer at the vicinity of the physical interface.

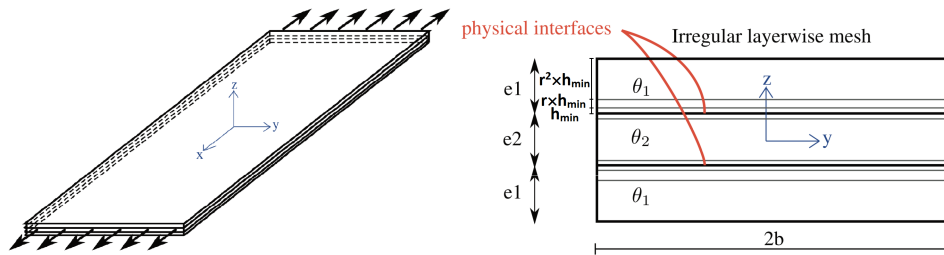


Figure 1. Multilayered plate refined through the thickness (irregular layerwise mesh).

3. Examples and numerical results

A new version of the in-house finite element code MPFEAP is dedicated to the SCLSI model. The element used is an 8-node isoparametric quadrilateral element with $6n-1$ d.o.f. per node, n being the number of layers of the laminates. This element has the same interpolation functions as the *LSI*'s element [6]. Next, comparisons are made between *LSI*, refined *LSI*, *SCLSI*, refined *SCLSI* and full 3D FE model (calculated using *ABAQUS* software) in order to evaluate the performances of the new model. A $(90^\circ, 0^\circ, 90^\circ)$ laminate under uniaxial tension is studied, the interlaminar shear stress is studied at a straight free-edge. For the first and third layer, the thickness is $e_1 = e_3 = 1\text{mm}$, the fiber orientation is 90° and the elastic constants are: $E_L=140\text{GPa}$, $E_T=E_N=15\text{GPa}$, $G_{LT}=G_{LN}=G_{TN}=5.85\text{GPa}$, $\nu_{LT}=\nu_{LN}=\nu_{TN}=0.21$; where L , T and N refer, respectively, to the fiber, transverse, and thickness direction. For the layer 2, the thickness is $e_2 = 0.8\text{mm}$, the fiber orientation is 0° and the elastic constants are: $E_L=160\text{GPa}$, $E_T=E_N=8.5\text{GPa}$, $G_{LT}=G_{LN}=4.1\text{GPa}$, $G_{TN}=2.8\text{GPa}$, $\nu_{LT}=\nu_{LN}=0.33$, $\nu_{TN}=0.5$.

The considered laminate is a plate with a length of $2l$ and a width of $2b$, respectively in the x and y directions (Fig. 2). The thickness of the laminate following z direction is equal to $2h = 2e_1 + e_2$ and the middle plane of the plate is located at $z=0$. Uniform displacements $\pm\Delta$ in the x direction are imposed at

the edges $x = \pm l$ where the applied overall strain in x axis is $\Delta/l = 0.05$, while the other edges remain free. The dimension $2b$ is set to 56mm, whereas the plate is assumed to be so long in the x direction ($l \gg b$) that the stress, strain components are independent of the x -coordinate far from the ends $x = \pm l$. As a consequence, instead of modeling the whole plate, it is sufficient to use only one finite element in the x direction, the size of this element in the x axis direction being irrelevant.

In this example, the normal stress σ_{33} is singular at the $90^\circ/0^\circ$ interface near the free edges, while the shear stress σ_{23} is null at the free edges and very highly concentrated in the vicinity of these edges. In Abaqus 3D FE, the element used is C3D8R (3D, 8-node, linear, isoparametric element with reduced integration). In order to obtain accurate results, a very strong mesh refinement is applied near the free edges and at the interfaces between layers. Element sizes in y and z axis follow geometric progressions and the smallest elements are located at the intersection of the free edges with the interfaces between layers. The smallest element size in y and z axis direction are set to $Y = 0.71\mu\text{m}$ and $Z = 7.5\mu\text{m}$, respectively.

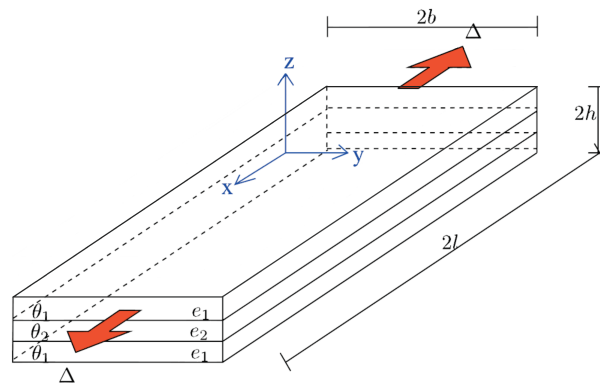


Figure 2. Laminate geometry, imposed displacements and coordinate system.

3.1. Comparison between 3D FE, SCLS1 and LS1 refined and non refined models

The refined *SCLS1* model is studied. Recall that there are two additional parameters in this model: p , the number of mathematical layers per physical layer, and the thickness of the smallest mathematical layer h_{min} . Choosing $h_{min} = 80\mu\text{m}$ in layer 2, a parametric study on p has been performed. It can be seen in Fig. 3 that the convergence is quickly reached for $p \geq 3$. In the light of the parametric study

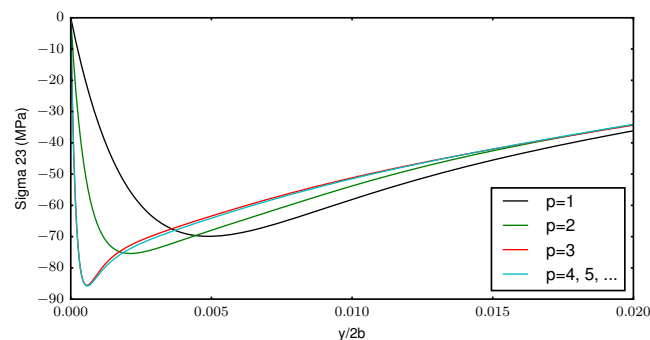


Figure 3. Zoom near the free edge on the distribution of the interlaminar shear stress σ_{23} predicted by the refined *SCLS1* model, for $e_2/h_{min} = 10$ and different values of p .

conducted in [13], it can be concluded that the best mesh strategy for the refined models is to use $p = 3$ and $h_{min} = e_2/10$ for the refined *SCLS1* model, and $p = 4$ and $h_{min} = e_2/10$ for the *LS1* model.

Excerpt from ISBN 978-3-00-053387-7

In Fig. 4, we plot the distribution of the interlaminar shear stresses σ_{23} at the $90^\circ/0^\circ$ interface between layer 1 and 2 as predicted by 3D FE (FE^- in the 90° layer and FE^+ in the 0° layer), LSI , refined LSI with $h_{min} = 80\mu m$ in layer 2 and $p = 4$, $SCLSI$ and refined $SCLSI$ with $h_{min} = 80\mu m$ in layer 2 and $p = 3$. It is seen that the refined $SCLSI$ model is the only model which can efficiently predict both stress concentration and free boundary condition. It must be highlighted that even if the refined LSI model doesn't comply with the exact 3D boundary conditions at free edges, nevertheless, it predicts the stress concentration with good accuracy (10%).

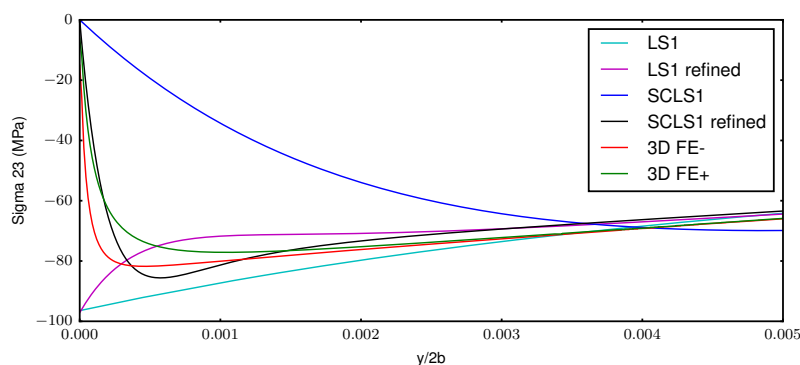


Figure 4. Zoom near the free edge on the distribution of the interlaminar shear stress σ_{23} predicted by the refined and non refined LSI and $SCLSI$ models and by the 3D FE model.

4. Conclusion

In this paper, a new statically compatible layerwise stress model for laminated plates called $SCLSI$, has been presented. As in the LSI model initially proposed in [1], the laminated plate is considered as a superposition of Reissner plates coupled by interlaminar stresses which are considered as generalized stresses. However, the divergences of the interlaminar transverse shears are introduced as additional generalized stresses in the $SCLSI$ model. Also a *refined* version of the new model is obtained by introducing several mathematical layers per physical layer. In addition, an 8-node isoparametric quadrilateral FE with $6np - 1$ d.o.f. at each nodal point has been formulated. The FE program called MPFEAP has been updated in order to take into account the new model. The proposed new FE program presents a 2D type data structure that provides several advantages over a conventional 3D FE model: simplified input data, ease of results' interpretation, very big reduction of calculation time and interlaminar stresses are given in a straightforward manner without any post-processing work. When considering the number of d.o.f., the refined $SCLSI$ model has $6np - 1$ d.o.f. in the thickness direction to be compared to $3N$ where N is the number of FE nodes in thickness direction (N was up to 200); the d.o.f. for the refined $SCLSI$ model ($p=3$ and $n=3$) are more than 10 times less than for Abaqus 3D FE. As well, the performance of the new element has been compared with a 3D FE for free edge problem: the proposed $SCLSI$ model has better performance because it is able to reproduce both stress concentration and free edge boundary conditions at a reduced cost. Besides, although the refined LSI model cannot comply with the exact free edge boundary conditions, it can still be considered as an acceptable approximation of the $SCLSI$ model and thus of the 3D model, for the prediction of stress concentration near free edge boundaries.

Regarding future work, it would be interesting to extend the $SCLSI$ model to the case where the interfaces between layers are not perfectly bonded showing an elasto-plastic behavior.

References

- [1] T. Naciri, A. Ehrlacher, and A. Chabot. Interlaminar stress analysis with a new multiparticle modelization of multilayered materials (m4). *Composites Science and Technology*, 58:337–343, 1998.
- [2] N. J. Pagano. Stress fields in composite laminates. *International Journal of Solids and Structures*, 14:385–400, 1978.
- [3] R.P. Carreira, J.F. Caron, and A. Diaz Diaz. Model of multilayered materials for interface stresses estimation and validation by finite element calculations. *Mechanics of Materials*, 34(4):217 – 230, 2002.
- [4] A. Diaz Diaz, J. F. Caron, and R. P. Carreira. Software application for evaluating interfacial stresses in inelastic symmetrical laminates with free edges. *Composite Structures*, 58:195–208, 2002.
- [5] J. F. Caron, A. Diaz Diaz, R. P. Carreira, A. Chabot, and A. Ehrlacher. Multi-particle modelling for the prediction of delamination in multi-layered materials. *Composites Science and Technology*, 66:755–765, 2006.
- [6] V. T. Nguyen and J. F. Caron. A new finite element for free edge effect analysis in laminated composites. *Computers and Structures*, 84:1538–1546, 2006.
- [7] J. Dallot and K. Sab. Limit analysis of multi-layered plates. part II: Shear effects. *Journal of the Mechanics and Physics of Solids*, 56:561–580, 2008.
- [8] N. Saeedi, K. Sab, and J. F. Caron. Delaminated multilayered plates under uniaxial extension. part I: Analytical analysis using a layerwise stress approach. *International Journal of Solids and Structures*, 49:3711–3726, 2012.
- [9] N. Saeedi, K. Sab, and J. F. Caron. Delaminated multilayered plates under uniaxial extension. part II: Very efficient layerwise mesh strategy for the prediction of delamination onset. *International Journal of Solids and Structures*, 49:3727–3740, 2012.
- [10] N. Saeedi, K. Sab, and J. F. Caron. Cylindrical bending of multilayered plates with multi-delamination via a layerwise stress approach. *Composite Structures*, 95:728–739, 2013.
- [11] A. Lerpiniere, J.F. Caron, A. Diaz Diaz, and K. Sab. The LS1 model for delamination propagation in multilayered materials at $0^\circ/\theta^\circ$ interfaces: A comparison between experimental and finite elements strain energy release rates. *International Journal of Solids and Structures*, 51:3973–3986, 2014.
- [12] E. Carrera. On the use of the murakami’s zig-zag function in the modeling of layered plates and shells. *Computers and Structures*, 82:541–554, 2004.
- [13] R. Baroud, K. Sab, J. F. Caron, and F. Kaddah. A statically compatible layerwise stress model for the analysis of multilayered plates. *International Journal of Solids and Structures*, submitted.